

Regaining Loss in Dynamic Stability after Control Surface Failure for an Air-Breathing Hypersonic Aircraft Flying At Mach 8.0

Zairil A. Zaludin

Department of Aerospace Engineering, Universiti Putra Malaysia, Selangor, Malaysia
E-mail: zairil_azhar@upm.edu.my

(Received 22 March 2021; Revised 19 April 2021; Accepted 15 May 2021; Available online 22 May 2021)

Abstract - The aim of the study is to reconfigure the automatic flight control systems of a hypersonic vehicle so that dynamic stability can be restored when flight control fails. LQR theory is used to first find the feedback gain when all 3 flight control systems are working. Failure was simulated one at a time to investigate lost in dynamic stability. When instability occurs, the new gains are obtained for the remaining flight controls using a modified Minimum Principle theory. The simulations show that the dynamic stability can be restored using these new reconfiguration gains if any one of the 3 flight control systems fail at one time but not in combination. The failure of elevator flaps at hypersonic speeds is likely due to aerodynamic heating. It is shown that the engine diffuser and the temperature across combustor controls can regain longitudinal dynamic stability to at least slow down the aircraft to safety. Study is limited to longitudinal motion only.
Keywords: Hypersonic Vehicle Dynamics, Control Reconfiguration, LQR Theory, Minimum Principle

I. INTRODUCTION

A situation may arise in flight when one or more of the aircraft control inputs becomes inoperative. To avoid the potential loss of the Hypersonic Transport Aircraft (HST) aircraft due to the instability which can result as a consequence of this loss in control, it is necessary to have available another closed-loop control system which will be capable of restoring the dynamic stability by using the other control surfaces or excursions which are still functioning. Such a technique is referred to as reconfiguration control.

HST is a vision of the aviation future, which started since the 1950's with the launch of the X-15 hypersonic programs. That idea has recently been kept in the fore front of aviation with the publication of a NASA contracted report entitled 'Independent Market Study: Commercial Hypersonic Transportation' [1]. Various articles in magazines such as [2,3,4]. Unlike aircraft flying at supersonic speeds, aircraft attempting or attempted to fly at hypersonic speeds have faced many technical challenges. A few of these problems have been highlighted in [1] again, 50+ years after the first flight of X-15. This implies that those problems still have no solution or proven solutions for hypersonic vehicle to fly safely at hypersonic speeds.

One of the challenges highlighted in [1] is the need to accept the highly likelihood that HST aircraft primary flight control surfaces will not be effective when flying at high

hypersonic speeds. In addition to that, it is also highly likely that when deflected, the heat generated from the air friction will likely damage the control surfaces as no material have yet been found that can sustain such temperatures generated due to aerodynamic heating. But flying a hypersonic aircraft will not involve flying at hypersonic speeds only. These flight control surfaces are still required for flight phases involving subsonic and supersonic speeds. Hence, these flight control surfaces will still be used onboard the aircraft, but it is expected that these flight control surfaces will be used together with Reaction Jet Controls (RJC) for better effectiveness. The control surfaces will still be used.

Because of this, some work has been done on systems that could tolerate failure of the hypersonic flight control systems. [5] proposed a solution to abrupt actuator faults by circumventing unwanted effects of the faulty actuators through estimating the lower bounds of the gain faults and the upper bounds of the bias faults. In [6], a passive fault tolerant control scheme was proposed in the presence of actuator fault. It was shown in that work that not only the benefits of both incremental control and twisting control are inherited, but their side effects were also reduced. In [7], a fault tolerant control law (FTC) was proposed consisting of improved integral sliding mode (ISM) equivalent law, a power reaching law, and a new adaptive compensation control law. In that work, the FTC showed fast convergence speed and expected attitude tracking performance. The work done in [8] specifically focused on faulty rudder on the hypersonic vehicle and investigated the use of hybrid FTC. In [9], the authors proposed an adaptive control scheme for hypersonic vehicle experiencing actuator failures. 2 adaptive fault tolerant controllers were designed for velocity subsystem and altitude system. By using the controllers, flight states containing the angle of attack, flight path angle, pitch angle and pitch angle rate could be guaranteed in prospective ranges.

The novelty of the work presented in this paper is the regaining of the aircraft fundamental stability – the dynamic stability. The work here shows that when a HST flying at Mach 8 at 85,000ft with Stability Augmentation System (SAS) engaged, the dynamic stability of the aircraft would be compromised when the elevator control surface completely malfunction. The other 2 remaining controls, the temperature across combustor, T_o , and duct area ratio, A_D ,

failed to sustain the dynamics stability of the aircraft after the total loss of elevator control surface. But when the aircraft use the new proposed reconfigured feedback gain, both T_o and A_D managed to sustain the aircraft dynamic stability. When the aircraft responses were investigated, the transitions of control authority to the remaining controls occurred without drastic effects on the responses. It was interesting to observe that for this aircraft flying at such high speed as Mach 8 at 85,000ft, the dynamic stability could be sustained well using the remaining controls. The regaining of dynamic stability would allow the pilots or

autopilot system to at least slow down the aircraft to a safer speed and land for inspections. The work done is focused on longitudinal motion only.

II. THE VEHICLE

For convenience of reference, the name **HYPERION** has been given by the present authors to this mathematical model. A sketch of this hypothetical aircraft is shown in Fig. 1.

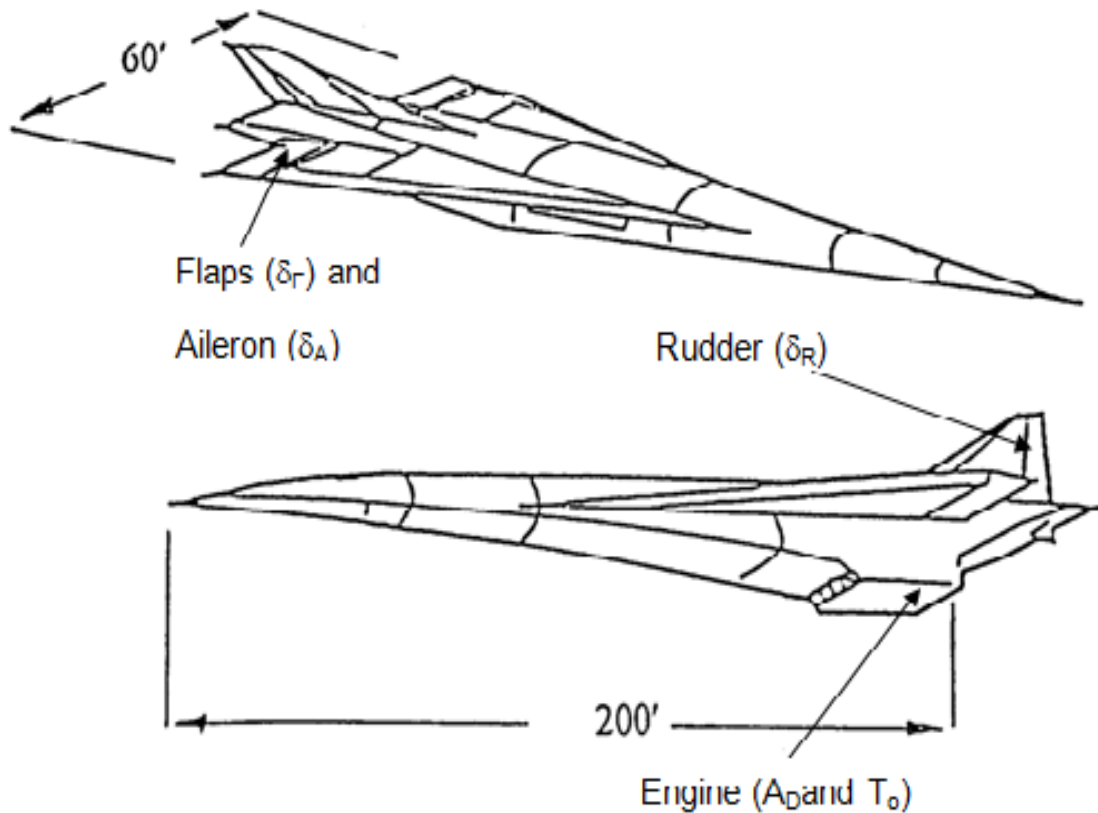


Fig. 1 The Generic Hypersonic Aircraft Sketch

The mathematical model was linear and has five control inputs, viz.:

δ_F denoting flap surface deflection.

A_D denoting the ratio of engine diffuser area.

T_o denoting the temperature across the engine combustor.

δ_A denoting aileron deflection.

δ_R denoting rudder deflection.

The first three controls are used for controlling longitudinal motion and the final two are used for controlling the aircraft lateral motion. Hyperion concept is based on the work by Chavez and Schmidt [10]. These authors conducted a thorough analysis of the mathematical model of the

hypersonic aircraft on a two-dimensional representation which is shown as Fig. 2.

By using this two-dimensional model, two important features simplify the analysis of the dynamic characteristics of the aircraft: a forebody compression surface and an afterbody/nozzle expansion surface. The lower forebody compression surface serves as a lifter and acts as an external diffuser for the engine. The vehicle afterbody and nozzle surfaces serve as external expansion nozzles which produce both thrust and lift. In Table I are the aircraft geometry data used for all the mathematical models of the longitudinal motion considered in this paper.

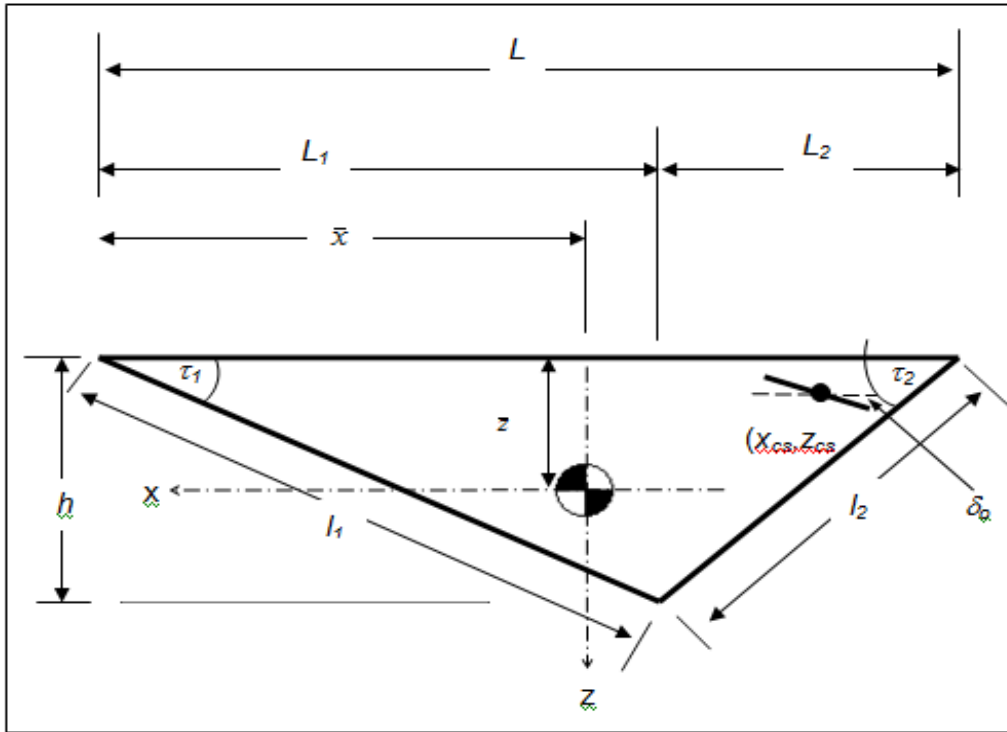


Fig. 2 Two-dimensional representation and geometrical details of the HST vehicle

TABLE I AIRCRAFT GEOMETRY DATA

Aircraft Geometry			
τ_1	=0.24435 rad (14°)	δ_o	=0.52395 rad (30.02°)
τ_2	=0.34907 rad (20°)	h	=22.20 ft
L	=150 ft	$\Delta \tau_1$	=1.7453 × 10 ⁻² rad (1°)
L_1	=89.02ft	$\Delta \tau_2$	=1.7453 × 10 ⁻² rad (1°)
L_2	=60.98 ft	m	=500 slug/ft
$\frac{S_{cs}}{b}$	=22.5ft	m	=40 slug/ft
\bar{x}	=90.00 ft	g	=32.2 ft/s ²
\bar{z}	=11.25 ft	I_{yy}	=1.0 × 10 ⁶ slug ft ² /ft
x_{cs}	=-52.50 ft	ω_1	=18 rad/s
z_{cs}	=-11.25 ft	ζ_1	=0.02
l_1	=91.756 ft	l_2	=64.894 ft

I_{yy} is the inertia per unit width about the Y-axis, S_{cs} is the control surface reference area, ω_1 is the frequency of the first in-vacuo vibration mode, ζ_1 is the damping ratio of first in-vacuo vibration mode, m is vehicle mass per unit width, and m is the generalised elastic mass per unit width.

III. LONGITUDINAL MOTION OF AN HYPERSONIC TRANSPORT AIRCRAFT

The mathematical model of longitudinal motion used in this article was developed from an initial model based on that developed by Chavez and Schmidt [10]. Basically, the

integrated modelling approach was used whereby contributing vector components (from three main sources; aerodynamic, propulsion and aeroelastic effects) were added to represent the forces in the X-axis direction, and the Z-axis direction and the total moment, M , about the centre of mass of the aircraft. A set of stability and control derivatives resulted from this analysis.

In the work reported here, the model of Chavez and Schmidt had to be modified to permit the investigation of the dynamic stability of the aircraft at Mach numbers above 8.0 and at heights above 85000ft i.e during the scramjet-phase of the flight mission.

Without a closed-loop control system Hyperion has been shown to be dynamically unstable [11]. A SAS was designed which stabilised the motion. Now, several different combinations of types of control input failures

were simulated to study the effect of different types of control input malfunction on the stability of the closed-loop aircraft dynamics. A technique of reconfiguring the closed-loop system by using the remaining active controls to recover stability was then considered subsequently.

IV. METHODOLOGY

A. The Mathematical Model of the Longitudinal Motion

The mathematical model used was represented by a linear, time-invariant, state equation:

$$\dot{\mathbf{x}} = \mathbf{A}\mathbf{x} + \mathbf{B}\mathbf{u} \quad (1)$$

$\mathbf{x} \in \mathbb{R}^n$ represents the state vector and $\mathbf{u} \in \mathbb{R}^m$ represents the control vector. \mathbf{A} is the state coefficient matrix and \mathbf{B} is the driving matrix, of order $(n \times n)$ and $(n \times m)$ respectively. If, for example, the aircraft dynamics has 7 state variables and 3 control variables, then $n = 7$ and $m = 3$. The state and the control variables are defined in Eqn (2) and Eqn (3). viz.

$$\mathbf{x} = \begin{bmatrix} \Delta u \text{ (ft/s)} \\ \Delta \alpha \text{ (rad)} \\ \Delta q \text{ (rad/s)} \\ \Delta \theta \text{ (rad)} \\ \Delta h \text{ (ft)} \\ \Delta \eta \text{ (rad)} \\ \Delta \dot{\eta} \text{ (rad/s)} \end{bmatrix} \quad (2)$$

$$\mathbf{u} = \begin{bmatrix} \Delta \delta_F \text{ (rad)} \\ \Delta A_D \\ \Delta T_o \text{ (oR)} \end{bmatrix} \quad (3)$$

The state variables are the forward speed u , the angle of attack α , the rate of change of the pitch attitude q , the pitch attitude θ , the height h , the bending displacement η and the rate of change of bending displacement $\dot{\eta}$. The variables are all perturbations from an equilibrium flight condition.

The output equation can be represented by:

$$\mathbf{y} = \mathbf{C}\mathbf{x} + \mathbf{D}\mathbf{u} \quad (4)$$

where $\mathbf{y} \in \mathbb{R}^p$. The output matrix, \mathbf{C} , is of order $(p \times n)$ and \mathbf{D} is of order $(p \times m)$. Often not all state variables in the aircraft dynamics are measurable. For example, if only three of the seven state variables are measurable, then $p = 3$.

B. Dynamic Stability of an Aircraft

The dynamic stability of the aircraft corresponding to the mathematical model was assessed by examining the eigen values of the corresponding coefficient matrix, \mathbf{A} , of the state-space equation [12]. Eigen values of the aircraft without any stability augmentation, λ , were obtained by solving the linear equation

$$\det[\lambda\mathbf{I} - \mathbf{A}] = 0 \quad (5)$$

\mathbf{I} is an identity matrix. Any aircraft is dynamically unstable if any of its eigen values has a positive real part.

C. Stabilisation of the Longitudinal Motion of Hyperion

The method of designing an effective SAS for Hyperion to stabilise the aircraft dynamics based on Linear Quadratic Regulator (LQR) theory is described in this section. The mathematical model was represented by Eqn (1).

D. Important Features of LQR Theory for Stability Augmentation

Using LQR theory, an optimal feedback control law can be obtained which guarantees the dynamic stability of the controlled aircraft. A performance index is minimised subject to the constraint of Eqn (1).

The performance index used in this work is given as Eqn (6).

$$\mathbf{J} = \frac{1}{2} \int_0^{\infty} (\mathbf{x}^T \mathbf{Q} \mathbf{x} + \mathbf{u}^T \mathbf{G} \mathbf{u}) dt \quad (6)$$

The superscript, T , indicates the transpose of the matrix.

The state-weighting matrix, \mathbf{Q} , is of order $(n \times n)$ and the control-weighting matrix, \mathbf{G} , must be of order $(m \times m)$. The resulting optimal linear feedback control law can be shown to be:

$$\mathbf{u}^o = -\mathbf{K}\mathbf{x} \quad (7)$$

where the feedback gain matrix, \mathbf{K} , is defined as:

$$\mathbf{K} = \mathbf{G}^{-1} \mathbf{B}^T \mathbf{P} \quad (8)$$

\mathbf{P} is the solution obtained from solving the corresponding algebraic Riccati equation. \mathbf{P} is a symmetrical positive definite matrix. The algebraic Riccati equation is:

$$\mathbf{P}\mathbf{A} + \mathbf{A}^T \mathbf{P} - \mathbf{P}\mathbf{B}\mathbf{G}^{-1} \mathbf{B}^T \mathbf{P} + \mathbf{Q} = 0 \quad (9)$$

The dynamic stability of an aircraft with closed-loop control can be determined by solving Eqn (10). A controlled aircraft is dynamically stable if all the real eigenvalues of the closed-loop eigenvalues or the real parts of these eigenvalues are negative.

$$\det[\zeta\mathbf{I} - (\mathbf{A} - \mathbf{B} \times \mathbf{K})] = 0 \quad (10)$$

In this research work, a Computer Aided Engineering (CAE) software package (called Matlab) was used, together with its associated Control System Toolbox, to obtain the solution, P, to the Riccati matrix equation, the feedback control matrix, K, and also the closed-loop eigenvalues of the system.

Three conditions must be satisfied when using the package to solve any LQR problem. These theoretical requirements are commonly stated in the literature as

1. The matrix, G, must be positive definite.
2. The matrix, Q, must be at least positive semi-definite.
3. The system of Eqn (1) must be completely controllable.

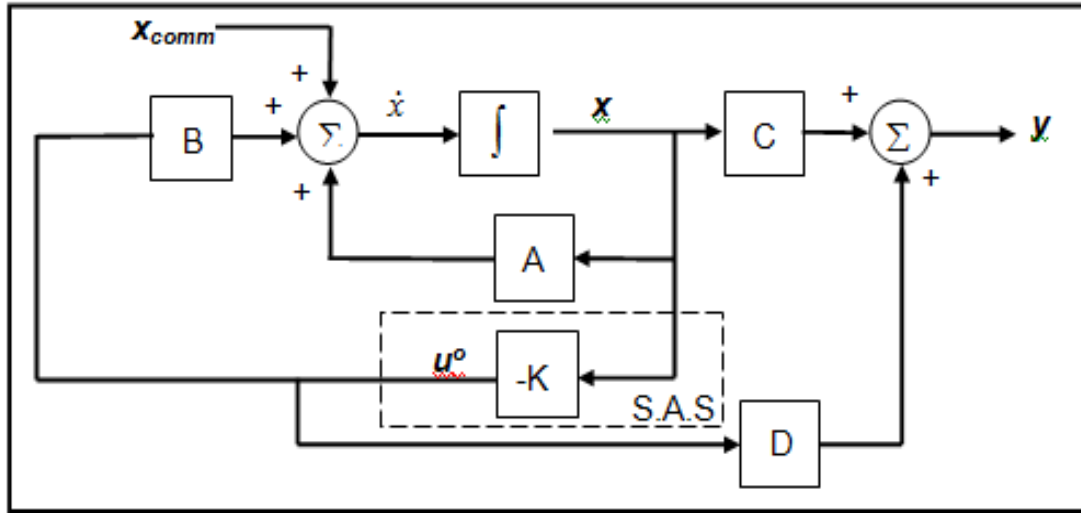


Fig. 3 Aircraft dynamics with a Stability Augmentation System (SAS)

x_{comm} is the command input for the controlled aircraft dynamics, and is a vector of dimension, n. The state equation for the closed-loop system now becomes,

$$\dot{x} = (A - BK)x + x_{comm} \quad (11)$$

and the output equation,

$$y = (C - DK)x \quad (12)$$

E. A Method to Reconfigure a Closed-Loop Control System

By using LQR theory, an unstable aircraft can be stabilised. An optimal control law like Eqn (7) can then be used to provide stabilisation. But when a control failure occurs, this closed-loop control law requires modification so that stability can be regained using the control inputs that are still active [13].

To account for control failures, Eqn (7) should be re-written as:

$$u_R = -K_D K_{FB} x \quad (13)$$

Note here that the control vector u_R is of order $(m \times 1)$ and x , the state vector is of order $(n \times 1)$. u_R represents a reconfiguration control vector and K_D a control distribution matrix. K_{FB} is the feedback gain matrix. If the control reconfiguration is perfect, then,

$$K_D K_{FB} = K \quad (14)$$

where K is the optimal feedback gain matrix obtained when all control inputs of the aircraft are operating.

Hence, a perfect reconfiguration system will ensure that:

$$B_F u_R = B u^o \quad (15)$$

Here B is the original driving matrix of the aircraft without control input failure, and B_F is the driving matrix of the state equation of the aircraft with one or more of the control inputs inoperative. Those columns of B_F which correspond to the failed control inputs are null. Note that the case being considered here is complete failure of the control.

Next, let K_{DO} denote the no-failure distribution matrix and K_{DR} denote the reconfiguration control distribution matrix. Both matrices are square and of order $(m \times m)$. Without any control input failure

$$K_{DO} = K_D \quad (16)$$

In Eqn (5.2), K is of order $(m \times n)$. If K_{FB} is also of order $(m \times n)$, then K_{DO} will be square and of order $(m \times m)$. To obtain K_{FB} , K_{DO} is taken to be some convenient, but arbitrary matrix. So, from Eqn (14),

$$K_{DO} \cdot K_{FB} = K \quad (17)$$

ie. perfect reconfiguration is assumed. If K_{DO} is chosen to be an identity matrix, then,

$$K_{FB} = K \tag{18}$$

It should be noted that the choice of K_{DO} is arbitrary so that it need not necessarily be an identity matrix to achieve the required distribution for stability. K_{DR} can be found by minimising a quadratic matrix function, L , using the ‘Minimum Principle’ [12]. Suppose the function, L , to be minimised is written as:

$$L = (B_F \cdot K_{DR} - B \cdot K_{DO})^T \cdot Z \cdot (B_F \cdot K_{DR} - B \cdot K_{DO}) + K_{DR}^T \cdot M \cdot K_{DR} \tag{19}$$

Those persistent and large errors which exist between the responses of the no-failure control system and that of the reconfigured control system are penalised by the weighting matrix, Z , of order $(n \times n)$. The size of the elements in K_{DR} is constrained by the weighting matrix, M , of order $(m \times m)$.

From Eqn (19),

$$\frac{\partial L}{\partial K_{DR}} = 0 \tag{20}$$

Hence,

$$K_{DR} = (B_F^T \cdot Z \cdot B_F + M)^{-1} B_F^T \cdot Z \cdot B \cdot K_{DO} \tag{21}$$

Using these matrices K_{DR} and K_{FB} , the eigenvalues, κ , of the reconfigured control system can be found by solving Eqn (22). i.e.

$$\det[\kappa I - (A - B_F K_{DR} K_{FB})] = 0 \tag{22}$$

where $i = 1, 2, 3 \dots n$

The objective of the reconfiguration system is to drive the closed-loop eigenvalues of the aircraft with control failure to be as close to, if not identical to, those obtained when there is no control failure, i.e:

$$\det[\kappa I - (A - B_F K_{DR} K_{FB})] = \det[\zeta I - (A - BK)] \tag{23}$$

Incidentally, when any control input suddenly becomes inoperative, then the eigenvalues of the aircraft with the faulty control input can be found using the corresponding matrix, B_F , associated with the control input failure, viz.

$$\det[\zeta I - (A - B_F K)] = 0 \tag{24}$$

The block diagram of the aircraft dynamics with the control reconfiguration system is represented in Fig. 4.

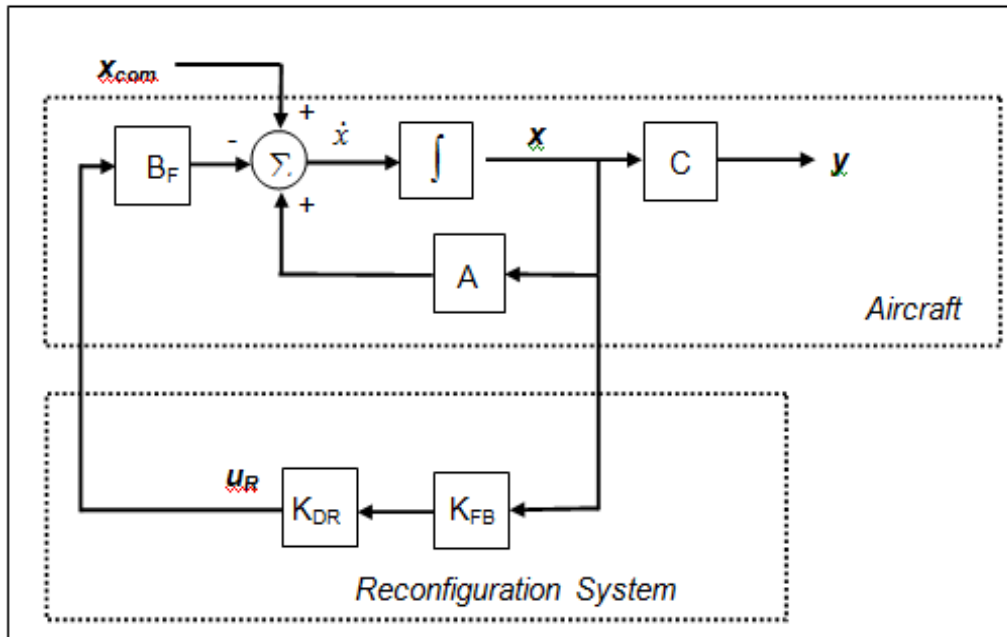


Fig. 4 Aircraft dynamics with a control reconfiguration system

The matrices that can be selected by the designer when reconfiguring the aircraft control system are K_{DO} , Z and M . Of course, the designer also has the choice of selecting the matrices, Q and G , used to minimise the performance index Eqn (6) for initial stabilisation of the aircraft without control failure. It is shown in the next section that using different matrices Z and M can achieve the desired stable reconfigured aircraft.

V. RESULTS AND DISCUSSION

This section of the paper contains results from 4 dynamic stability situations that would be shown by the hypersonic vehicle during flight at hypersonic speeds. In these tests, the aircraft was simulated flying at Mach 8.0 at a height of 85000ft. The situations are as follows.

1. The dynamic stability without any assistance from the Stability Augmentation System.
2. The dynamic stability with the assistance from the Stability Augmentation System.
3. The dynamic stability when control surface completely fails but aircraft is assisted by the same Stability Augmentation System when all controls were working
4. The implementation of Reconfiguration System to regain control to regain dynamic stability closed to before failure occurred. To regain the loss of control with least change to flight dynamics performance to the

aircraft is ideal. This hypersonic vehicle is travelling at Mach 8 hence, even if the dynamic stability could be regained, if the acceleration change caused due to the failure was huge, the prospect of structural failure is likely and the whole exercise to recover the aircraft flight stability deemed useless.

From the derivation of mathematical model, the matrices A and B for Hyperion flying at Mach 8 at an altitude of 85,000ft was found to be as follows:

$$A = \begin{bmatrix} -4.1857 \times 10^{-3} & -35.03 & 0.4269 & -32.2 & 7.9938 \times 10^{-4} & 18.614 & 0.4301 \\ -2.3158 \times 10^{-6} & -5.8716 \times 10^{-2} & 1.0002 & 0 & 4.4227 \times 10^{-7} & -3.9534 \times 10^{-2} & 2.1974 \times 10^{-4} \\ -9.4647 \times 10^{-6} & 4.3430 & -5.7885 \times 10^{-2} & 0 & 1.8076 \times 10^{-6} & 7.2990 & -5.2846 \times 10^{-2} \\ 0 & 0 & 1 & 0 & 0 & 0 & 0 \\ 0 & -7.8487 \times 10^3 & 0 & 7.8487 \times 10^3 & 0 & 0 & 0 \\ 0 & 0 & 0 & 0 & 0 & 0 & 1 \\ 1.4938 \times 10^{-3} & 54.953 & -0.41812 & 0 & -2.8529 \times 10^{-4} & -269.05 & -1.1340 \end{bmatrix} \quad (25)$$

$$B = \begin{bmatrix} -1.1359 \times 10^2 & -1.7159 \times 10^2 & 1.3329 \times 10^{-2} \\ -1.4513 \times 10^{-2} & 4.7726 \times 10^{-3} & -1.672 \times 10^{-7} \\ -2.3511 & -8.2859 \times 10^{-1} & 6.909 \times 10^{-5} \\ 0 & 0 & 0 \\ 0 & 0 & 0 \\ 0 & 0 & 0 \\ 0 & -9.8249 \times 10^{-1} & 3.4421 \times 10^{-5} \end{bmatrix} \quad (26)$$

To study the effect of loss in flight control surfaces or engine parameters, the performance of the aircraft when all control surfaces and engine parameters are working properly are determined first. Comparison can be made later if any changes has occurred because of the failure. Of

particular interest to the work here is the dynamic stability of the hypersonic aircraft and the implications to the aircraft dynamic responses with respect to time. When no SAS is incorporated into the aircraft flight dynamics, the aircraft eigen values obtained are shown in Table 2.

TABLE II HYPERION OPEN-LOOP EIGENVALUES, NATURAL MODE FREQUENCIES AND DAMPING RATIOS THE AIRCRAFT DYNAMICS CORRESPONDED TO HYPERION FLYING AT MACH 8.0 AND AT A HEIGHT OF 85000FT

Open - Loop Eigenvalues	Natural Frequencies	Damping Ratios	Motion Represented
$\lambda_{1,2} = -0.00189 \pm j0.0578$	0.058 rad/s	0.03	Phugoid
$\lambda_{3,4} = -0.55 \pm j16.4$	16.4 rad/s	0.03	Structural Bending
$\lambda_5 = -2.49$	-	-	Short Period
$\lambda_6 = 2.33$	-	-	Short Period
$\lambda_7 \rightarrow 0$	-	-	Height

When any aircraft is subjected to a command or disturbances, the induced short period mode shows significant changes in the angle of attack and the pitch rate [14]. Without any S.A.S, Hyperion showed highly unstable short period motion (See Table I).

for the performance index given in Eqn (6) are presented below.

$$Q = \text{diag}[1.0 \ 5.0 \ 10.0 \ 0.1 \ 1 \times 10^{-5} \ 0.0 \ 0.0] \quad (27)$$

$$G = \text{diag}[1.0 \ 1.0 \ 1.0] \quad (28)$$

How LQR theory was used to obtain an optimal feedback control law which stabilised the aircraft dynamics is described next. The matrices, Q and G, which were chosen

The choice of the elements for the matrix, Q, was made to stabilise the short period mode.

High penalties were placed on any changes in the angle of attack, $\Delta\alpha$, (e.g. in Eqn (27); $Q(2,2) = 5.0$) and the pitch rate, Δq ($Q(3,3) = 10.0$). This choice of weighting elements was made to penalise any persistent motions involving these state variables. At this time, no penalty was applied to any changes in structural bending, $\Delta\eta$ and $\Delta\dot{\eta}$ because the contributions of these variables towards the aircraft instability were uncertain. The other diagonal elements of the matrix, Q , were chosen completely arbitrarily. The three

controls, δ_F , A_D and $T_{o\text{use}}$ on Hyperion were penalised equally as can be seen from the matrix, G , of Eqn (28). Note that the matrix, Q , was positive semidefinite; the matrix, G was positive definite as required by the LQR theory published in most of the literature.

A solution to the associated Riccati equation was found from use of a routine in the Matlab Control System Toolbox. The resulting matrix was

$$P = \begin{bmatrix} 0.005 & 0.593 & -0.043 & -0.708 & -3.8 \times 10^{-5} & -0.008 & -0.001 \\ 0.593 & 3555.1 & -69.1 & -3852.4 & -0.244 & -13.98 & -2.149 \\ -0.043 & -69.1 & 4.61 & 81.58 & 0.005 & 0.891 & 0.115 \\ -0.708 & -3852.4 & 81.58 & 4200.3 & 0.263 & 16.09 & 2.49 \\ -3.8 \times 10^{-5} & -0.244 & 0.005 & 0.263 & 2.6 \times 10^{-5} & 0.0009 & 0.0001 \\ -0.008 & -13.98 & 0.891 & 16.09 & 0.0009 & 0.91 & 0.02 \\ -0.001 & -2.149 & 0.115 & 2.49 & 0.0001 & 0.02 & 0.0059 \end{bmatrix} \quad (29)$$

This solution, P , to the algebraic Riccati equation is both symmetrical and positive definite. Using Eqn (8), the

optimal feedback gain matrix can then be calculated. It is shown below as Eqn (30).

$$K^T = \begin{bmatrix} -0.505 & -0.86 & 6.7 \times 10^{-5} \\ 43.57 & -25.33 & 0.002 \\ -4.99 & 3.05 & -0.0002 \\ -55.48 & 33.03 & -0.003 \\ -0.003 & 0.002 & -1.6 \times 10^{-7} \\ -0.996 & 0.524 & -4.0 \times 10^{-5} \\ -0.119 & 0.07 & -5.7 \times 10^{-6} \end{bmatrix} \quad (30)$$

From Eqn (10), all the closed-loop eigen values of the optimally controlled aircraft can be deduced to possess negative real parts which indicates that the controlled

aircraft will be dynamically stable. After stabilisation the eigen values of Hyperion were found and are shown in Table III.

TABLE III HYPERION'S CLOSED-LOOP EIGENVALUES FLYING AT MACH 8.0 AND AT A HEIGHT OF 85000FT

Closed - Loop Eigen values	Natural Frequencies	Damping Ratios	Motion Represented
$\zeta_{1,2} = -0.52 \pm j0.6$	0.79 rad/s	0.66	Phugoid
$\zeta_{3,4} = -0.55 \pm j16.428$	16.4 rad/s	0.03	Structural Bending
$\zeta_5 = -5.765$	-	-	Short Period
$\zeta_6 = -205.87$	-	-	Short Period
$\zeta_7 = -1.3288$	-	-	Height

A. Flaps Inoperative

If the flaps of Hyperion completely fail, the first column of the matrix, B , is set to null. The other 2 columns represent

A_D and T_o are still active controls for Hyperion. Using Eqn (22), the closed-loop eigen values of the faulty aircraft were found and compared with those of the controlled aircraft without control failure.

$$B_F = \begin{bmatrix} 0 & -1.7159 \times 10^2 & 1.3329 \times 10^{-2} \\ 0 & 4.7726 \times 10^{-3} & -1.672 \times 10^{-7} \\ 0 & -8.2859 \times 10^{-1} & 6.909 \times 10^{-5} \\ 0 & 0 & 0 \\ 0 & 0 & 0 \\ 0 & 0 & 0 \\ 0 & -9.8249 \times 10^{-1} & 3.4421 \times 10^{-5} \end{bmatrix} \quad (31)$$

TABLE IV CLOSED-LOOP EIGENVALUES FOR AIRCRAFT WITHOUT AND WITH FLAPS OPERATING

Closed-loop eigen values for aircraft with flaps operating			Closed-loop eigen values for aircraft with flaps inoperative		
$\zeta_{1,2}$	=	$-0.52 \pm j0.6$	$\zeta_{1,2}$	=	$-0.0006 \pm j0.0555$
$\zeta_{3,4}$	=	$-0.55 \pm j16.428$	$\zeta_{3,4}$	=	$-0.55 \pm j16.428$
ζ_5	=	-5.765	ζ_5	=	-2.5538
ζ_6	=	-205.87	ζ_6	=	-145.37
ζ_7	=	-1.3288	ζ_7	=	2.4414 (Unstable)

From these eigen values, it is evident that the aircraft has become dynamically unstable with the loss of flap control, since ζ_7 is a positive real root. The optimal feedback gain matrix, K, for the faulty aircraft has to be reconfigured if closed-loop stability is to be recovered.

To obtain K_{DR} , the following matrices were used:

$$K_{DO} = \text{diag}[1 \ 1 \ 1] \quad (32)$$

$$Z = \text{diag}[1 \ 1 \ 1 \ 1 \ 1 \ 1 \ 1] \quad (33)$$

$$M = \text{diag}[1 \ 1 \ 1] \quad (34)$$

K_{DR} was found by solving Eqn (21) i.e.

$$K_{DR} = \begin{bmatrix} 0 & 0 & 0 \\ 6.6201 \times 10^{-1} & 9.9997 \times 10^{-1} & -7.7674 \times 10^{-5} \\ -8.7199 \times 10^{-5} & -7.7674 \times 10^{-5} & 7.8112 \times 10^{-9} \end{bmatrix} \quad (35)$$

Eqn (22) was solved for κ to find the eigen values of the reconfigured closed-loop system.

The closed-loop eigen values for the reconfigured aircraft were found to be

TABLE V CLOSED-LOOP EIGENVALUES FOR HYPERION WITH FLAPS INOPERATIVE

Closed-loop eigen values for aircraft with reconfigured system		
$\kappa_{1,2}$	=	$-0.0004 \pm j0.0555$
$\kappa_{3,4}$	=	$-0.55 \pm j16.428$
κ_5	=	-2.55
κ_6	=	-205.69
κ_7	=	2.39 (Unstable)

Note that one of the short period mode eigen values was unstable. The short period mode eigen values for the uncontrolled aircraft were known to correspond to dynamic instability and it appears that with the flaps inoperative, it is impossible to recover the dynamic stability of the controlled aircraft. However, choosing different matrices, Z and M, had an impact on recovering the stability of the control-affected system.

$$Z = \text{diag}[1 \ 100 \ 10 \ 100 \ 1 \ 0 \ 0] \quad (36)$$

$$M = [0] \quad (37)$$

$$K_{DR} = \begin{bmatrix} 0 & 0 & 0 \\ -28.5445 & 1 & 0 \\ -3.7599 \times 10^5 & -1.3119 \times 10^{-6} & 1 \end{bmatrix} \quad (38)$$

Using different matrices, Z and M, such as those denoted by Eqn (36) and (37), resulted in the reconfigured aircraft becoming dynamically stable. The matrix, K_{DR} , calculated using these matrices is shown in Eqn (38).

The closed-loop eigen values of the reconfigured system are shown in Table VI. From inspection, it is obvious that the closed-loop system with reconfiguration is stable for this specific control-input failure.

TABLE VI CLOSED-LOOP EIGENVALUES FOR RECONFIGURED HYPERION WITH FLAPS INOPERATIVE

Closed-loop eigen values from using the K_{DR} matrix Eqn (35)	Closed-loop eigen values from using the K_{DR} matrix Eqn (38)
$\kappa_{1,2} = -0.0004 \pm j0.0555$	$\kappa_{1,2} = -0.116 \pm j3.024$
$\kappa_{3,4} = -0.55 \pm j16.428$	$\kappa_{3,4} = -0.631 \pm j16.272$
$\kappa_5 = -2.55$	$\kappa_5 = -2.93$
$\kappa_6 = -205.69$	$\kappa_6 = -205.7493$
$\kappa_7 = 2.39$ (Unstable)	$\kappa_7 = -0.449$ (Stable)

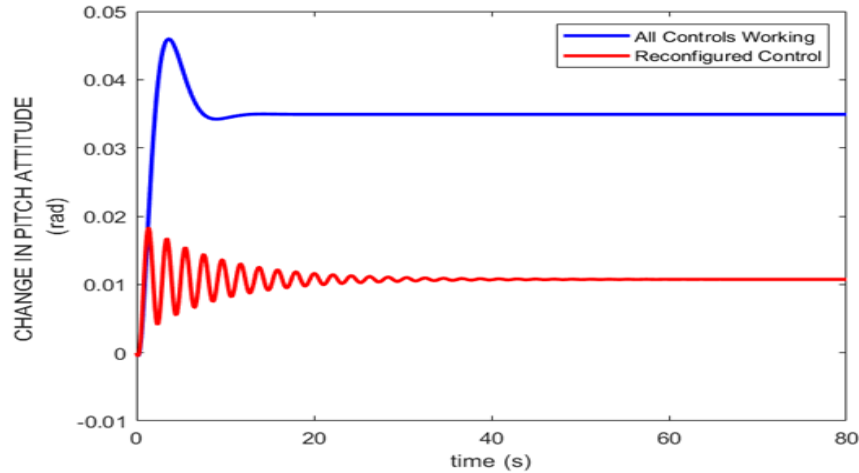


Fig. 5 The changes in pitch attitude responses of Hyperion without δ_f failure ($\Delta\theta$) and with δ_f failure plus reconfiguration system ($\Delta\theta_{reconf}$)

The change in pitch attitude ($\Delta\theta$) responses of the aircraft to a commanded step input in pitch attitude of 2° (0.0349 radian) is shown in Fig. 3.

That the aircraft dynamic stability is stable can be seen from the responses shown in Figure 3. However, the steady-state value of the change in pitch attitude from the reconfigured aircraft differs from that produced by aircraft without control failure. This means that the reconfiguration system was unable to perfectly reconstruct the aircraft closed-loop dynamics to provide the same response before the control failure occurred. The error between the steady-state values, was approximately 0.025 radian. Note also that the phugoid mode oscillation in the response of the reconfigured aircraft

showed a period of oscillation of 2.1 seconds and a damping ratio of 0.04 but when the flaps were operating, the phugoid motion was visible but showed a lower frequency of oscillation of 0.8 rad/s and a damping ratio of 0.65. $\Delta\theta$ response completely settled after 9 seconds whereas $\Delta\theta_{reconf}$ showed the phugoid oscillation up to 43 seconds before settling. A similar oscillation was observed in the responses of the other state variables. However, these oscillations settled after approximately 40 seconds of simulation time.

In Fig. 4 is shown the change in height (Δh) response of the aircraft when it was subjected to a commanded step change in height of 1000ft.

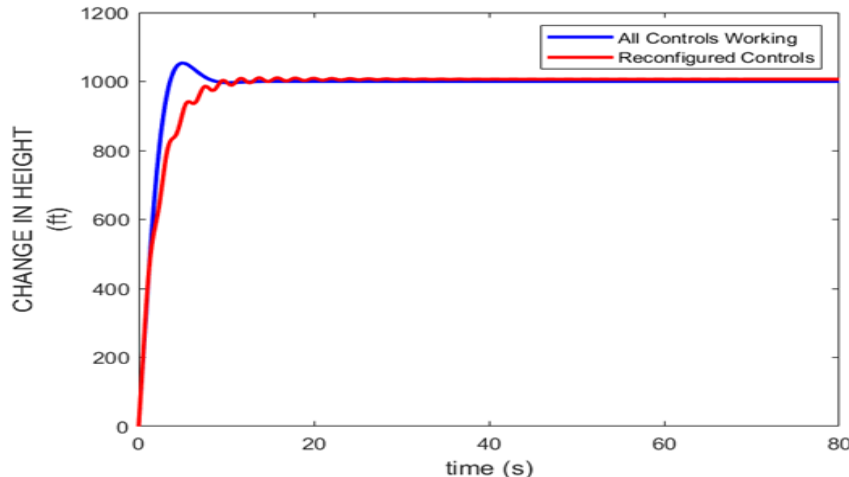


Fig. 6 The change in height responses with δ_f operating (Δh) and with δ_f inoperative plus reconfiguration system (Δh_{reconf})

For a commanded step change in height of 1000ft, there was little difference (6.3ft) in the steady-state height responses between the aircraft with and without the reconfiguration system. The phugoid oscillation is again visible in the

response of the aircraft with the reconfiguration system but it settled in about 25 seconds. The normal acceleration response at the centre of gravity (C.G) of the aircraft to the same command, was also simulated, and is shown in Fig.7

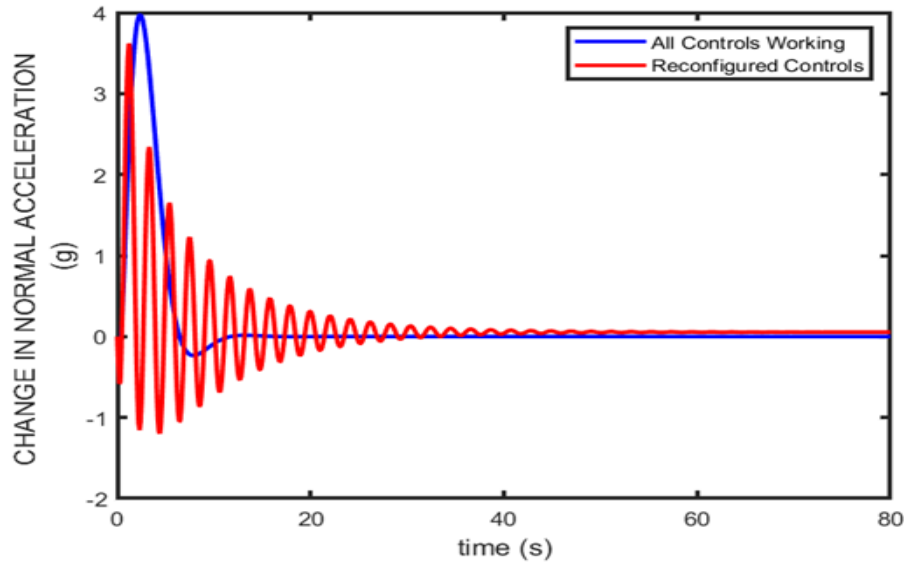


Fig. 7 The change in normal acceleration responses at the aircraft C.G with δ_F operating (Δn_z) and with δ_F inoperative plus reconfiguration ($\Delta n_{z_{reconf}}$)

In summary, when this aircraft is flying at a speed of Mach 8 at 85,000ft, the aircraft was shown to be dynamically unstable but with the incorporation of a Stability Augmentation System, the dynamic stability could be established. If the aircraft control flaps completely malfunction at Mach 8, the aircraft is shown to lose this stability even though the SAS is still incorporated. But by reconfiguring the feedback gains, K, of the SAS using the

technique shown here, the dynamic stability of the aircraft could be regained. The response tests conducted on the aircraft shows that the change in state variables is relatively small during the configuration process.

The results of the control reconfiguration tests conducted using Hyperion longitudinal motion are summarised in Table VII.

TABLE VII SUMMARY OF THE CONTROL RECONFIGURATION SYSTEM PERFORMANCE

Types of Control Failures	Unstable after failure	Stable after reconfiguration
δ_F	✓	✓
A_D	✓	✓
T_o	✓	Not required
δ_F and A_D	✓	✗
δ_F and T_o	✓	✗
A_D and T_o	✓	✗

VI. CONCLUSION

In this paper, the results are presented for a study of a reconfigurable closed-loop control system for Hyperion when one or more of the aircraft control inputs are inoperative. The objective of the reconfiguration system was to regain at least the same degree of aircraft dynamic stability if any of the control inputs fail. Using the method, the optimal feedback gain matrix obtained for the aircraft without any control inoperative was distributed appropriately. By using this distribution matrix, the work effort of the affected control surface is distributed to the other control surfaces which were still operating. There are three matrices, K_{DO} , Z and M , which can be chosen by the

designer to design a reconfiguration system that will fully recover the aircraft's lost stability. The tests conducted to confirm the effectiveness of the reconfiguration system at first involved the longitudinal motion of Hyperion. The aircraft was assumed to be flying at Mach 8.0 and at a height of 85000ft. Using the method discussed, the aircraft dynamic stability could be recovered after δ_F failed. Using the 2 remaining controls on the aircraft, both from the air-breathing scramjet engine, it is shown in this paper that the longitudinal dynamic stability is not compromised. Dynamic stability was also regained when A_D failed leaving only δ_F and T_o operational. It was learned also from the study that when T_o failed, no lost in dynamic stability was observed hence, no reconfiguration of controls required.

REFERENCES

- [1] C. Mullins and R. Lehmer, "Commercial Hypersonic Transportation Market Study," NASA Contractor or Grantee Report, May 1 2021, Document ID: 20210015471. [Online]. Available: <https://ntrs.nasa.gov/citations/20210015471>
- [2] G. Norris, *NASA Steps Up Civil Hypersonic Studies with Aerion, GE, Aviation Week*, 2021. [Online]. Available: <https://aviationweek.com/businessaviation/aircraft-propulsion/nasa-steps-civil-hypersonic-studies-aerion-ge>.
- [3] M. Dempsey, *Rival powers jockey for the lead in hypersonic aircraft*. BBC News, 2020. [Online]. Available: <https://www.bbc.com/news/business-53598874>.
- [4] K. Baggaley, *This hypersonic airliner would take you from Los Angeles to Tokyo in under two hours*. NBC News, 2019. [Online]. Available: <https://www.nbcnews.com/mach/science/hypersonic-airliner-would-take-you-los-angeles-tokyo-under-two-ncna1045986>.
- [5] S. Zhu, T. Xu, C. Wei, and Z. Whang, "Learning-based adaptive fault tolerant control for hypersonic flight vehicles with abrupt actuator faults and finite time prescribed tracking performance," *European Journal of Control*, Vol. 58, pp 17 -26, 2021.
- [6] T. Han, Q. Hu, HS. Shin, A. Tsourdos, and M. Xin, "Incremental Twisting Fault Tolerant Control for Hypersonic Vehicles with Partial Model Knowledge," *IEEE Transactions on Industrial Informatics*, 2021. [Online]. Available: <https://doi.org/10.1109/TII.2021.3080303>
- [7] F. Guo, P. Lu, "Improved Adaptive Integral-Sliding-Mode Fault-Tolerant Control for Hypersonic Vehicle with Actuator Fault," *IEEE Access*, Vol. 9, pp.46143-46151.2021. [Online]. Available: <https://doi.org/10.1109/ACCESS.2021.3067038>
- [8] KY. Hu, W. Li, and Z. Cheng, "Hybrid Adaptive Fault-Tolerant Control for Compound Faults of Hypersonic Vehicle," *IEEE Access*, Vol. 9, pp. 56927-56939. 2021. [Online]. Available: <https://doi.org/10.1109/ACCESS.2021.3066501>
- [9] JG. Sun, CM. Li, Y. Guo, CQ. Wang, and L. Peng, "Adaptive fault tolerant control for hypersonic vehicle with input saturation and state constraints," *Acta Astronautica*, Vol. 167, pp. 302-313, 2020.
- [10] F. R. Chavez, and D. K. Schmidt, "Analytical Aeropropulsive/Aeroelastic Hypersonic-Vehicle Model with Dynamic Analysis," *Journal of Guidance, Control and Dynamics*, Vol. 17, No. 6, pp. 1308-1319, 1994.
- [11] D. McLean and Z. A. Zaludin, "Stabilization of longitudinal motion of a hypersonic transport aircraft," *Transactions of the Institute of Measurement & Control*, Vol. 21, No. 2-3, pp. 99-105, 1999.
- [12] M. Athans, P. L. Falb, *Optimal Control - An Introduction to the Theory and Its Applications*, McGraw-Hill, NY, 1966.
- [13] D. McLean, and S. Aslam-Mir, "Reconfigurable Flight Control Systems," in IEE Control '91 Conference Edinburgh, Scotland, UK, Mar 25 -28, pp. 234-242.1991.
- [14] D. McLean, *Automatic Flight Control System*, Prentice Hall, Hemel Hempstead, U.K., 1993.